scientific reports

Check for updates

OPEN

Lattice dynamics in $CePd_2Al_2$ and $LaPd_2Al_2$

Petr Doležal[1]✉, Petr Cejpek[1], Satoshi Tsutsui[2,3], Koji Kaneko[4], Dominik Legut[5], Karel Carva[1] & Pavel Javorský[1]

The interaction between phonons and 4f electrons, which is forming a new quantum state (quasi-bound state) beyond Born-Oppenheimer approximation, is very prominent and lattice dynamics plays here a key role. There is only a small number of compounds in which the experimental observation suggest such a scenario. One of these compounds is $CePd_2Al_2$. Here the study of phonon dispersion curves of (Ce,La)Pd_2Al_2 at 1.5, 7.5, 80 and 300 K is presented. The inelastic X-ray scattering technique was used for mapping the phonon modes at X and Z points as well as in Λ and Δ directions, where the symmetry analysis of phonon modes was performed. The measured spectra are compared with the theoretical calculation, showing very good agreement. The measurements were performed in several Brillouin zones allowing the reconstruction of phonon dispersion curves. The results are discussed with respect to the magneto-elastic interaction and are compared with other cerium compounds. The phonon mode symmetry A_{1g} was found to be unaffected by the interaction, which is in contrast to previous assumptions.

Physical properties of intermetallic compounds are driven by their electronic properties and lattice dynamics, but usually their impact is treated separately. This is also the case of magnetism in rare earth compounds. The localised character of 4f electrons and their geometrical arrangement in the crystal lattice determine the magnetic behaviour and the lattice dynamics is usually not considered. This approach is based on the Born-Oppenheimer approximation, where the difference of several orders of magnitude in mass of atomic nucleus and electrons typically justify this attitude.

In standard crystal electrical field (CEF) theory the rare earth ion with full rotation symmetry is placed into a static crystal lattice, which decreases degrees of freedom and reduces the degeneracy of a ground state depending on the point symmetry of a given site in the crystal lattice. It was shown, that this approach cannot explain the magnetic excitation spectra measured in several compounds, e.g. in pyrochlores $Tb_2Ti_2O_7$[1], $Ho_2Ti_2O_7$[2], intermetallics $CeAl_2$[3], $PrNi_2$[4], $CePd_2Al_2$[5], $CeCuAl_3$[6] and recently in $CeAuAl_3$[7]. The Ce-based intermetallics have a very prominent position with a relatively small number of expected CEF excitations. The oxidation number of the Ce ion in the materials listed above is 3+, implying total angular momentum $J = \frac{5}{2}$ and a six fold degenerated ground state. The half integer moment requires at least two fold degeneracy even in triclinic site symmetry in the crystal lattice. This simply restricts the number of magnetic excitations from the ground state to two. The higher number of observed magnetic excitations in the spectra than two is very peculiar. One of the possible explanations of such behaviour was found in the coupling of lattice dynamics and 4f electronic states, which is usually neglected in the Born-Oppenheimer approximation as mentioned above. This would lead to the formation of a new quantum state[8] and opens new questions about its origin and conditions which have to be fulfilled. All these aspects make these compounds very interesting especially in the case when an X-ray free electron laser opens new possibilities to study the lattice dynamics.

The $CeAl_2$ crystallises in a cubic structure of type $MgCu_2$ Laves phase[9]. The site symmetry of the Ce ion is also cubic, therefore only two levels Γ_7^2 and Γ_8^4 (based on CEF theory) and one excitation from ground state are expected. Surprisingly, two excitations from the doublet Γ_7^2 have been observed by inelastic neutron scattering[3]. Simultaneously the study of phonon dispersion curves by inelastic neutron scattering shows a softening and broadening of the Γ'_{25} phonon mode and symmetry related phonon branches in the Λ direction[10]. Both observed features were explained by the existence of a quasi-bound state between 4f electrons and phonons[8]. The interaction term in the model Hamiltonian uses the crystal electrical field operator with the same transformation

[1]Faculty of Mathematics and Physics, Department of Condensed Matter Physics, Charles University, Ke Karlovu 5, 121 16 Prague 2, Czech Republic. [2]Japan Synchrotron Radiation Research Institute (JASRI), SPring-8, Sayo, Hyogo 679-5198, Japan. [3]Institute of Quantum Beam Science, Graduate School of Science and Engineering, Ibaraki University, Hitachi, Ibaraki 316-8511, Japan. [4]Materials Science Research Center, Japan Atomic Energy Agency, Tokai, Ibaraki 319-1195, Japan. [5]IT4Innovations, VSB-Technical University of Ostrava, 17. listopadu 2172/15, 708 00 Ostrava, Czech Republic. ✉email: Petr.Dolezal@karlov.mff.cuni.cz

properties as the Γ'_{25} mode[8]. This shows how the knowledge of phonon dispersion curves play a key role in search for the model Hamiltonian. Without direct observation of the influence of a quasi-bound state on phonons, the presence of the quasi-bound state remains still an open question.

The experimental studies in $CeCuAl_3$[6], $CePd_2Al_2$[5] and $CeAuAl_3$[7] propose the existence of a bound state, but its signature was found mainly in the magnetic excitations spectra. The study of phonon dispersion curves is still missing with some exception for $CeAuAl_3$ and $CeCuAl_3$[7,11]. The study of low energy phonon dispersion curves (mainly acoustic) on $CeAuAl_3$[7] shows the anticrossing of a non-dispersive magnetic excitation and an acoustic phonon branch, which was not observed before. The softening or broadening as known for $CeAl_2$ was not found in the measured energy interval[7].

Our present study of single crystal $CePd_2Al_2$ and $LaPd_2Al_2$ is focused on phonon dispersion curves studied by inelastic X-ray scattering. The non-magnetic La homologue is used as a reference sample, because the La ion have no 4f electrons and therefore the bound state between 4f electrons and phonons is not present here. We performed the symmetry analysis of phonon modes at Γ and X points and in the Δ and Λ directions, which were calculated in[12]. Based on the symmetry analysis we focused on selective phonon modes, especially with symmetry used in the model Hamiltonian[5] and compare it with the experimental data. The results are discussed in terms of a possible appearance of a quasi bound state in these Ce based intermetallics.

Methods

Single crystals of $CePd_2Al_2$ and $LaPd_2Al_2$ were prepared by the Czochralski method. As these compounds are incongruently melting, the procedure described in[13] was adopted. The starting compositions of the melted precursors were 22:41.1:36.9 (Ce:Pd:Al) and 22:39:39 (La:Pd:Al). The phase purity in the prepared ingots was checked by X-ray powder diffraction performed on Bruker D8 Advance diffractometer in Bragg-Brentano geometry with variable slits. The patterns of both Ce and La homologs were fit by a $CaBe_2Ge_2$ structural model using the Rietveld method with resulting lattice parameters $a = b = 4.4112(3)$ Å, $c = 9.8749(9)$ Å and $a = b = 4.439(1)$ Å, $c = 9.915(3)$ Å, respectively. The chemical composition was analysed by Energy-dispersive X-ray analysis and phase purity was also confirmed by backscattered electrons imaging performed on an electron microscope TESCAN, type Mira I LMH. The resulting composition of samples were 18:41:41 and 20:40:40 atomic precent of Ce:Pd:Al and La:Pd:Al. The measured chemical composition corresponds to ideal one within 2 % experimental error. The sample sizes of Ce and La based samples were 1 x 0.6 x 0.6 mm and 1 x 0.8 x 0.4 mm, respectively. The single crystalline samples were oriented by Laue method using a Laue X-ray Imaging System 20041209 SY Issue 8 (Photonic Science) with CCD camera (1220-1800 pixels) and air-cooled X-ray tube (30 kV, 300 μA). The beam size 0.5 mm^2 used for Laue method was smaller than the sample. A light-polarized microscopy was used to confirm the single-grain nature of the samples.

The previous study of polycrystalline $(Ce,La)Pd_2Al_2$ samples reveals the presence of a structural phase transition to a lower symmetry orthorhombic structure described by the *Cmme* (67) space group[5,14]. The temperature of the structural phase transitions, T_{str}, in prepared single crystals was checked by low temperature X-ray powder diffraction showing that the structural transitions are shifted to lower temperatures in comparison to the polycrystalline samples, $T_{str} \cong 6$ K for $CePd_2Al_2$ and $T_{str} \cong 60$ K for $LaPd_2Al_2$. In polycrystalline samples the transition temperatures were around 13.5 K (11 K) and 91.5 K (84 K)[5](14) for Ce and La samples, respectively. Details of the low temperature diffraction are presented in Supplementary information.

The inelastic X-ray scattering spectra were measured at the BL35XU beamline at the SPring-8 synchrotron (Japan). The high order 11 11 11 diffraction from a Si crystal and energy of 21.747 keV of the beam were used to ensure the energy resolution of 1.5 meV. The beam size was ≈ 50 μm. Si crystals were also used as analyser and their lattice parameters were controlled by a temperature, which allows the selection of the energy transfer. The detail description of BL35XU is given in[15,16].

Theoretical calculation of phonon dispersion curves in $(Ce,La)Pd_2Al_2$ are provided in[12]. For the analysis of inelastic spectra is necessary to know the polarisation and phase of displacement for all atoms in the primitive unit cell, which are given by eigenvectors $\mathbf{e}_{\mathbf{q}jd}$ and were calculated in[12]. The intensity of the selected phonon mode in a given Brillouin zone is proportional to dynamical structure factor, which one-phonon contribution is given by[16]:

$$S(\mathbf{Q},\omega)_{1p} = N \sum_{\mathbf{q}} \sum_{j} \left\| \sum_{d} \frac{f_d(\mathbf{Q})}{\sqrt{2M_d}} \quad e^{-W_d(\mathbf{Q})} \quad \mathbf{Q} \cdot \mathbf{e}_{\mathbf{q}jd} \quad e^{i\mathbf{Q}\cdot\mathbf{x}_d} \right\|^2 \delta_{(\mathbf{Q}-\mathbf{q})\boldsymbol{\tau}} \quad F_{\mathbf{q}j}(\omega), \tag{1}$$

where N counts the irradiated unit cells, $\boldsymbol{\tau}$ is the Bragg vector, $\mathbf{q}$ is the reduced momentum transfer in the first Brillouin zone, $\mathbf{Q} = \mathbf{q} + \boldsymbol{\tau}$. The index j runs over phonon modes for a given $\mathbf{q}$ and d runs over the atoms in the primitive unit cell. The position of atom within the unit cell is given by $\mathbf{x}_d$, M_d is its mass and f_d is the atomic form-factor for X-rays. $F_{\mathbf{q}j}(\omega)$ corresponds to the energy resolution function. $W_d(\mathbf{Q})) = B_d \frac{||\mathbf{Q}||^2}{16\pi^2}$ is the Debye-Waller factor. For our calculations, we use the Debye-Waller factor approximated for the case of isotropic vibrations[17] as:

$$B_d = \frac{6h^2}{M_d k_B \Theta_D} \left(\frac{\phi(\Theta_D/T)}{\Theta_D/T} + \frac{1}{4} \right) \tag{2}$$

where T is the temperature, Θ_D is Debye temperature and h and k_B are Planck and Boltzmann constant respectively. ϕ is the Debye function $\phi(x) = \frac{1}{x} \int_0^x \frac{\xi}{e^{\xi}-1} d\xi$.

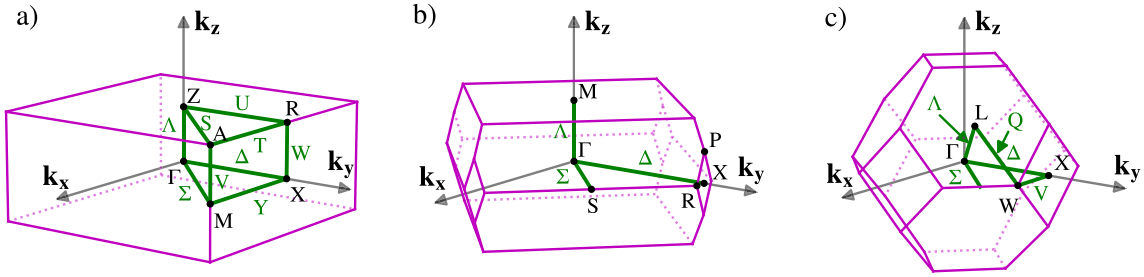

Figure 1. First Brilliouin zones and labels of higher symmetry points and directions, with respect to[18]. (**a**) Simple tetragonal lattice ($CePd_2Al_2$). (**b**) Body centered tetragonal lattice ($CeCuAl_3$). (**c**) Reciprocal body centered cubic lattice ($CeAl_2$-direct face centered cubic).

The measurement was done in these Brillouin zones 0 1 8, 0 0 8, 0 1 12, 0 2 14, 4 0 1, 3 0 1 and 4 0 0. This selection was chosen to cover a wide range of phonon branches with special attention to the possible separation of mode intensities during the data analysis based on the performed simulation given by Equation 1.

Results – Phonon dispersion curves in $(Ce,La)Pd_2Al_2$

The vibrations of atomic nuclei in the crystal structure are described by normal modes, which form the phonon dispersion curves in the Brilliouin zone. These modes are classified and labelled according to irreducible representations (IRs) of the group of $\mathbf{k}$ vector (little group) $\mathcal{G}_\mathbf{k}$ contained in mechanical representation. Before finding IR of $\mathcal{G}_\mathbf{k}$ it has to be noted that we have symmorphic (SSG) and non-symmorphic space groups (NSG). In the case of SSG, all translations can be factorised, and the factor group $\bar{\mathcal{G}}_\mathbf{k}$ form a point group. Unlike SSG, the NSG contain glide planes and screw axes, and consequently the $\bar{\mathcal{G}}_\mathbf{k}$ is not isomorphic to a point group in general. This means that only at the Γ point, $\mathbf{k} = 0$, the decomposition into IRs of point groups is possible for both SSG and NSG. In the following text, the phonon modes and phonon branches are labelled according to the solid state notation used in[18]. Only at the Γ point, where the little group $\mathcal{G}_\mathbf{k}$ is identical to the point group, the notation used in chemistry is given in brackets. Away from the centre of the Brilliouin zone, the symmetry of phonon dispersion curves were determined by using the compatibility relations in[18].

The point group of the $P4/nmm$ space group is D_{4h}. For symmetry determination of the phonon dispersion curves at the Γ point, we used the direct product of equivalence representation and representation of the polar vector:

$$\left(5A_{1g} + 3A_{2u} + 2B_{2u}\right) \times \left(E_u + A_{2u}\right) = 5E_u + 5E_g + 5A_{2u} + 3A_{1g} + 2B_{1g}. \quad (3)$$

There are therefore 20 different phonon modes (30 with the consideration of degeneracy) at the Γ point. This is in agreement with the fact that 10 atoms are in the primitive unit cell of $CePd_2Al_2$. All the 30 modes are listed in the Supplementary material and labelled with a number (#No.) increasing with their energy. These numbers are used further in the text.

The aforementioned symmetry analysis allows us to separate the calculated phonon branches in[12] according to their symmetry within the Brilliouin zone. Figure 1a shows higher symmetry points and directions in the primitive tetragonal unit cell using the notation in[18]. Our measurements were performed in Λ and Δ directions. Our symmetry analysis, shown in Fig. 2, is therefore limited to these directions. The four panels highlight always one symmetry type of phonon branches and the rest of them are plot in half-transparent colour for the sake of clarity. The non-symmorphic nature (a glide plane in the basal plane) of our space group is responsible for the two fold degeneracy of modes at the X point, where always two phonon branches are stuck together and consequently their slope is not perpendicular to the Brilliouin zone boundary, see X_1 and X_2 phonon modes in Fig. 2. The glide plane is also responsible for the mixed character of longitudinal and transversal Δ_1 and Δ_2 branches. Only Δ_3 and Δ_4 are pure transversal with displacement in the x-direction. The Δ_1 and Δ_2 phonon branches with a mixed character often tend to cross each other, which leads to frequent anticrossings. The dispersion curves for $CePd_2Al_2$ and $LaPd_2Al_2$ are very similar. Most of them appear at higher energies for $CePd_2Al_2$ compared to $LaPd_2Al_2$. This can be understood if we consider that the $CePd_2Al_2$ unit cell has a smaller volume. The detailed discussion about differences in these two homologs together with partial density of states is presented in[12].

The aim of our experimental study is a mapping of the selected phonon dispersion curves and especially modes with the A_{1g} symmetry as this symmetry was assumed to be involved in the magneto-elastic coupling[5]. The A_{1g} phonon modes are present only at the Γ point, where we find three of them. Figure 3 shows the displacement amplitude of atoms in the unit cell for all three A_{1g} modes. The energy of the phonon mode, involved in the magneto-elastic coupling, should be comparable with the energy of magnetic excitation from ground state in the unperturbed level scheme based on standard CEF theory. Based on the magnetic excitations observed by inelastic neutron scattering[5], this restricts our attention to the A_{1g} mode at 12.8 meV with a dominant motion of Ce ions, see Fig. 3. Direct measurement of inelastic x-ray scattering at the Γ point is not possible, because of the strong elastic signal, therefore the measurements were performed in the close vicinity of the Γ point at $\mathbf{q} = (0.00, -0.05, 0.00)$. The 0 1 8 Brilliouin zone was selected for measurements as the calculated intensity of A_{1g} mode at 12.8 meV is dominant in the spectra in this zone. Figure 4a shows the temperature dependence of the Δ_1 phonon mode (#13) related by compatibility relations with the A_{1g} mode at 12.8 meV at the Γ point. The

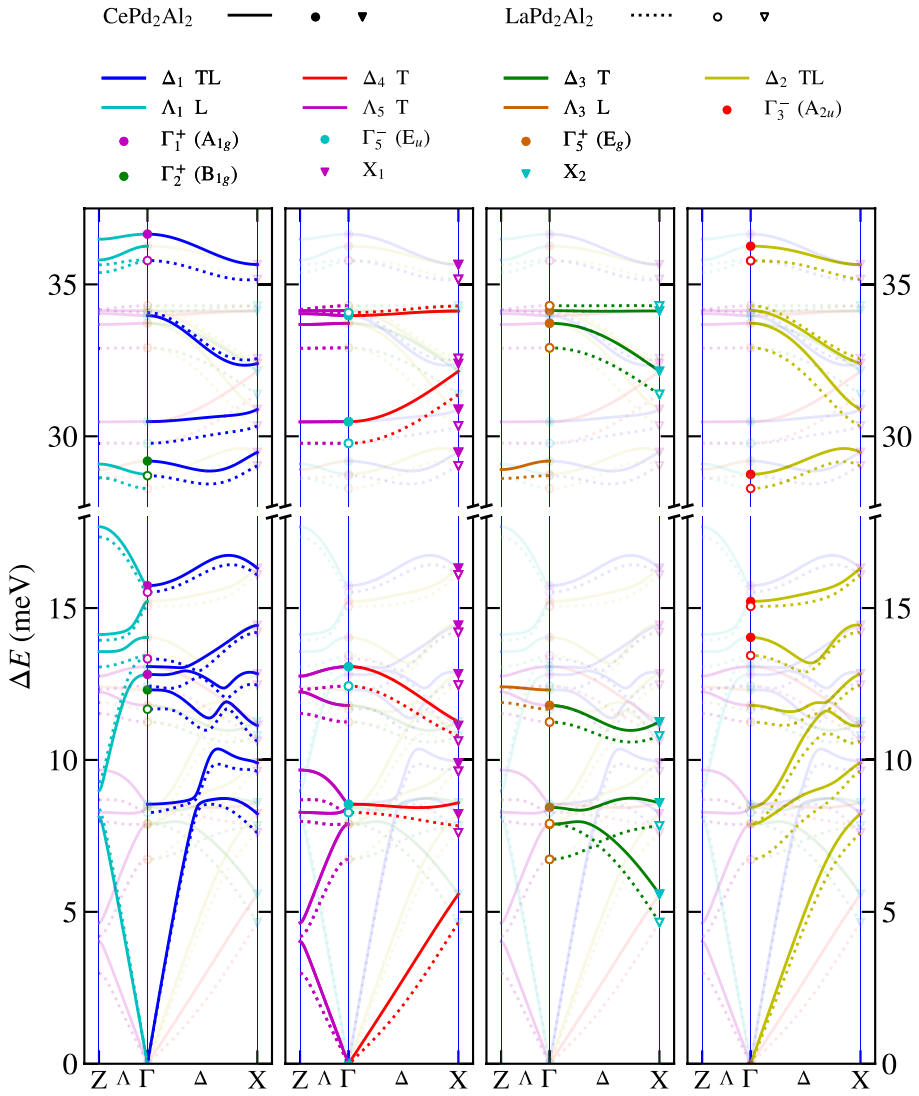

Figure 2. Symmetry analysis of 30 calculated phonon modes for (Ce,La)Pd_2Al_2, considering degeneracy. The abbreviation TL signifies the mixed character of longitudinal and transversal polarisation and T signifies a pure transversal character. Each panel highlight modes and branches with selective symmetry, the corresponding labels are above each panel. For details see chapter Results–Phonon dispersion curves in (Ce,La)Pd_2Al_2.

results are compared with calculated spectra in 4b. The measured spectra at the 0 1 8 Brillouin zone are almost identical for both $CePd_2Al_2$ and $LaPd_2Al_2$. The temperature dependence of the phonon mode energy is negligible with only a slight shift to higher energy at low temperature. The spectral width of modes is similar at room and lowest temperature and also for $CePd_2Al_2$ and $LaPd_2Al_2$ homologs.

The other phonon modes need also a closer inspections, since the magneto-elastic coupling in $CeAl_2$, which is the archetypal example, affects not only the given phonon mode, but the whole corresponding branches. From this point of view, it is important to study the **q** dependencies of phonon branches and compare them with the calculated ones and with non-magnetic analogues. It is almost impossible to find such a Brillouin zone, where only the intensity of one phonon branch will be intense and well separated from the others. This problem is partly solved by measuring at several Brillouin zones at the same **q** position. The energy of the phonon mode is then fitted and kept the same in all Brillouin zones. The spectral line shape is given by a pseudo-Voigt function, which parameters were determined by a fit of the elastic line. This procedure improves a lot the data analysis, but still the intensity ratio between modes based on a dynamical structure factor has to be fixed to increase the stability of the fit. The example of such procedure is shown in Fig. 5 for $CePd_2Al_2$ compound, $\mathbf{q} \approx (0.00, 0.24, 0.00)$ at 1.5 K. It has to be noted that the measured intensity is integrated intensity from a part of reciprocal space and not an intensity at given point in reciprocal space due to the finite resolution. This could have significant influence on the measured intensity, especially where the intensity of the mode changes rapidly within the Brillouin zone. This could also be the reason for enhanced intensity around 8 meV in the spectra, see Fig. 5. The same feature was observed for both Ce and La homologs (see comparison of measured data in Supplementary material) and cannot be therefore related to the magneto-elastic coupling.

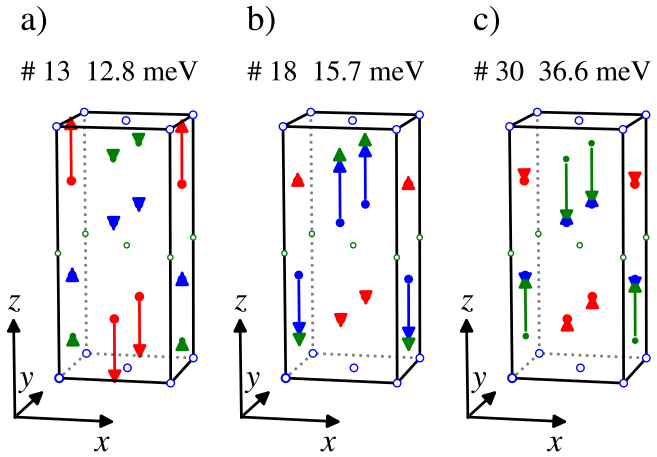

Figure 3. The atomic displacement of atoms for the Γ_1^+ (A_{1g}) phonon mode symmetry. Calculated at[12] for $CePd_2Al_2$. For clarity the displacement of each atom is 4 times enlarged. The labels #13 #18 #30 correspond to the notation used in Supplementary information, which labels the modes for a given **q** with increasing energy. The red, blue and green colours correspond to Ce, Pd and Al ions, respectively. The open circles represents static atoms in the mode.

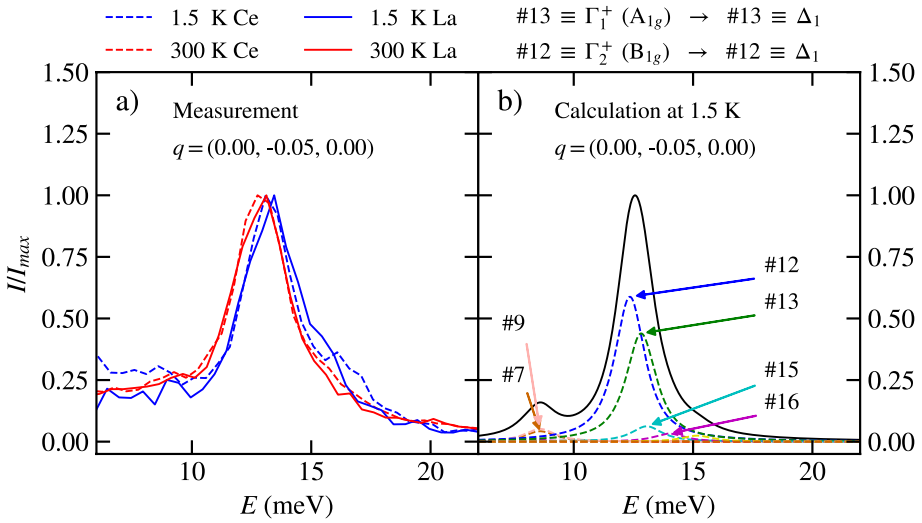

Figure 4. (**a**) The measured inelastic spectra at the 0 1 8 Brillouin zone ($\mathbf{q} = (0.00, -0.05, 0.00)$) temperatures 1.5 and 300 K. The results are shown for $CePd_2Al_2$ and $LaPd_2Al_2$ compounds. (**b**) The calculated intensity (full black line) is the sum of all 30 modes at the 0 1 8 Brillouin zone for $CePd_2Al_2$, the most intense modes are labelled.

The measurements were performed at three different temperatures 1.5, 7, and 280 K for $CePd_2Al_2$ and 1.5, 80 and 300 K for $LaPd_2Al_2$. The temperatures 7 and 80 K were selected to be close to the structural phase transition, but still above them. The results of the above mentioned analysis are shown in Figs. 6 and 7 for both Ce and La homologs, respectively. The **q**-dependences of phonon modes agree very well with the calculated ones. The temperature dependence of phonon energies is negligible, except the Δ_1 and Λ_1 branches around 15.7 meV, where the motion of Pd atoms is dominant. The significant difference between calculated and measured data is around 12.4 meV Δ_4 for $LaPd_2Al_2$, in contrary the results agree very well for $CePd_2Al_2$ in this symmetry. The raw measured data of Ce and La homologs are almost identical (see Supplementary material), which suggest better agreement between measurement and calculation for $CePd_2Al_2$. A significant shift of the Δ_2 branch to the higher energy of around 14.0 meV was observed for both compounds, although better agreement is found again for $CePd_2Al_2$.

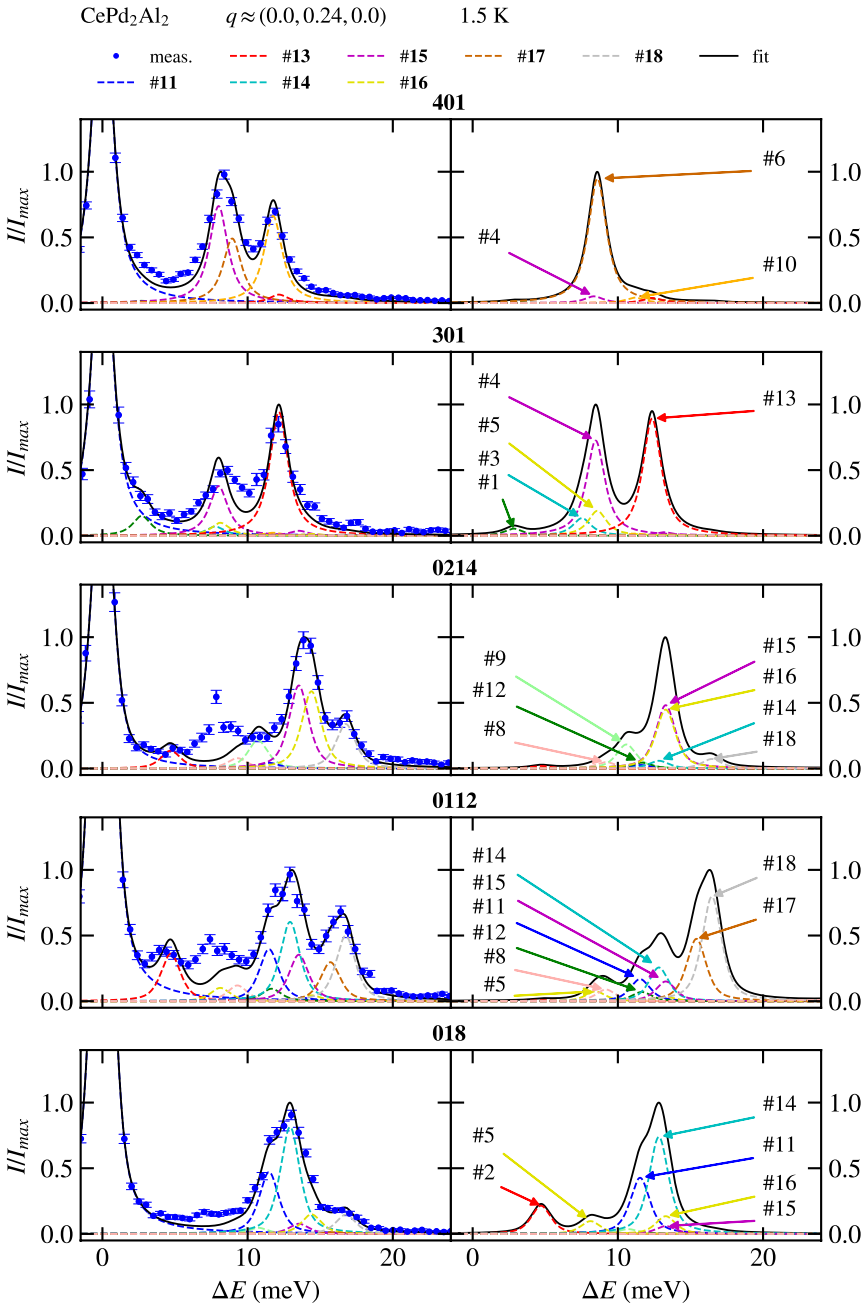

Figure 5. The fit of measured data at $\mathbf{q} = (0.00, 0.24, 0.00)$ on the left and calculated intensity based on dynamical structure factor on the right. Each pair of graphs correspond to the given Brillouin zone specified in bold above them. The most intense modes are labelled. The colour of the selected mode is the same across the Brillouin zones. The legend above shows modes of which energies were possible to determine conclusively.

Discussion – quasi-bound state

The phonon dispersion study in (Ce,La)Pd_2Al_2 is motivated by the proposed formation of a quasi-bound state in this compound. Therefore we discuss the experimental results with respect to the theoretical model describing this quantum state.

The CEF magnetic excitations are usually non-dispersive within Brillouin zone, unlike phonons. The strength of any magneto elastic coupling, g_0^{μ}, depends on $\boldsymbol{k}$ and on a given mode s. The most important contribution to the interaction term can be expressed as in[8]:

$$\hat{H}_{int} = -\sum_{l\tau}\sum_{\boldsymbol{k}s\mu} g_0^{\mu}(\boldsymbol{k}s,\tau)\left(\hat{a}_{\boldsymbol{k}s} + \hat{a}^{+}_{-\boldsymbol{k}s}\right)\hat{O}_{\mu}(\boldsymbol{R}_{l\tau})e^{-i\boldsymbol{k}\cdot\boldsymbol{R}_{l\tau}}, \tag{4}$$

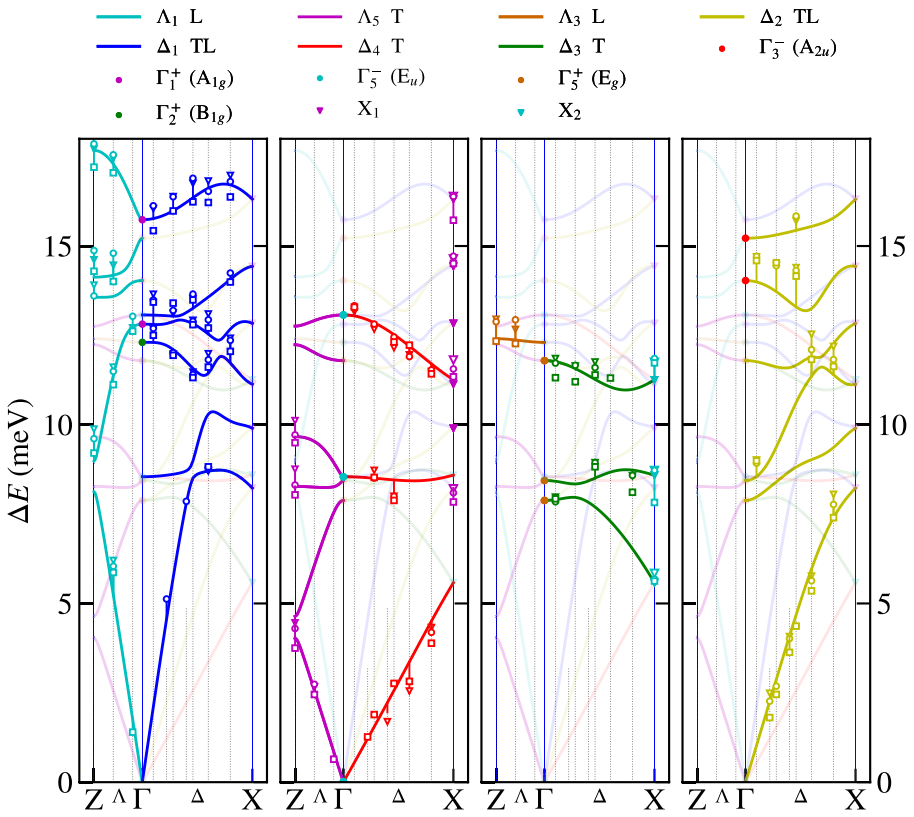

Figure 6. The comparison of theoretical calculation with the fit of measured inelastic X-ray scattering spectra for $CePd_2Al_2$ in energy range 0 - 17.5 meV. The □, ○, ▽ symbols correspond to 1.5, 7.5, 280 K, respectively. For details of the fit, see chapter Results – Phonon dispersion curves in $(Ce,La)Pd_2Al_2$.

where l, τ indexes run over primitive unit cell and atoms in the basis, respectively. The $\hat{a}$ and $\hat{a}^+$ are the annihilation and creation operators for phonons. The operator $\hat{O}_\mu$ represents CEF states and the $\hat{O}_\mu e^{-i\boldsymbol{k}\cdot\boldsymbol{R}_{l\tau}}$ should transform as the phonon mode $\boldsymbol{k}s$ (as the IR of little group). The $\hat{O}_\mu$ itself then transforms like IRs of a factor group of the little group. The factor group is a point group in case of SSG, while it is not generally isomorphic to a point group in case of NSG, see chapter Results - Phonon dispersion curves in $(Ce,La)Pd_2Al_2$. This has a consequence that the direct finding of $\hat{O}_\mu$ operators for some high symmetry points in the Brillouin zone is not possible in NSG. The situation is much easier at the Γ point ($\boldsymbol{k} = 0$), where the little group is a point group for SSG and also NSG. This simplification is used in the non-dispersive model for the interaction term[8]:

$$\hat{H}_{int} = -\sum_{\mu} g_\mu \left(\hat{a}_\mu + \hat{a}_\mu^+\right)\hat{O}_\mu, \tag{5}$$

where $\hat{a}_\mu^+$ and $\hat{a}_\mu$ are creation and annihilation operators for phonons μ, g_μ is a magnetoelastic coupling parameter. This interaction term was used for theoretical description in $CeAl_2$[8], $CeCuAl_3$[6], $CeAuAl_3$[7] and $CePd_2Al_2$[5].

Determination of the magneto-elastic coupling for various phonon modes and the decision about the dominant contribution is a highly non-trivial task. In the case of cubic $CeAl_2$ (the first Brillouin zone is shown in Fig. 1c this was assisted by experimental studies of phonon dispersion curves. Softening and broadening of the Γ'_{25} phonon mode was observed there, suggesting this mode to be considered in the model[10]. Such a direct observation of a quasi-bound state in the phonon dispersions of $CePd_2Al_2$, $CeCuAl_3$ and $CeAuAl_3$ has not been reported, yet.

Before we turn to our results on $CePd_2Al_2$, lets briefly discuss the case of $CeCuAl_3$ and $CeAuAl_3$. The previous single crystal studies of the phonon spectra in these two compounds were not focused on specific phonon modes with symmetry considered in the theoretical model. The crystal structure of $CeAuAl_3$ was determined to be the $BaNiSn_3$ structural type[19] with $I4$ mm space group. The space group is symmorphic and the point group is C_{4v}. The interaction term of model Hamiltonian uses the $\hat{O}_2^2 = \hat{J}_x^2 - \hat{J}_y^2$ operator[7]. This means that the corresponding phonon modes should transform as $x^2 - y^2$ basis function, which corresponds to the Γ_3 (B_1) phonon mode. Away from the Γ point, using the dispersive model, such symmetry could be found in V, M points and Λ direction, because the corresponding factor groups are isomorphic to the C_{4v} point group, see Fig. 1b. The crystal structure of $CeCuAl_3$ is often reported the same as that of $CeAuAl_3$, so the conclusions based on symmetry analysis would be valid also here. However the crystal structure of $CeCuAl_3$ seems to be more complex than $CeAuAl_3$. The partial site mixing on Cu and Al Wyckoff position was previously observed[19–21]. The model of a quasi-bound state is based on the fact, that Ce ions in the crystal structure have identical environments, which is not expected for the

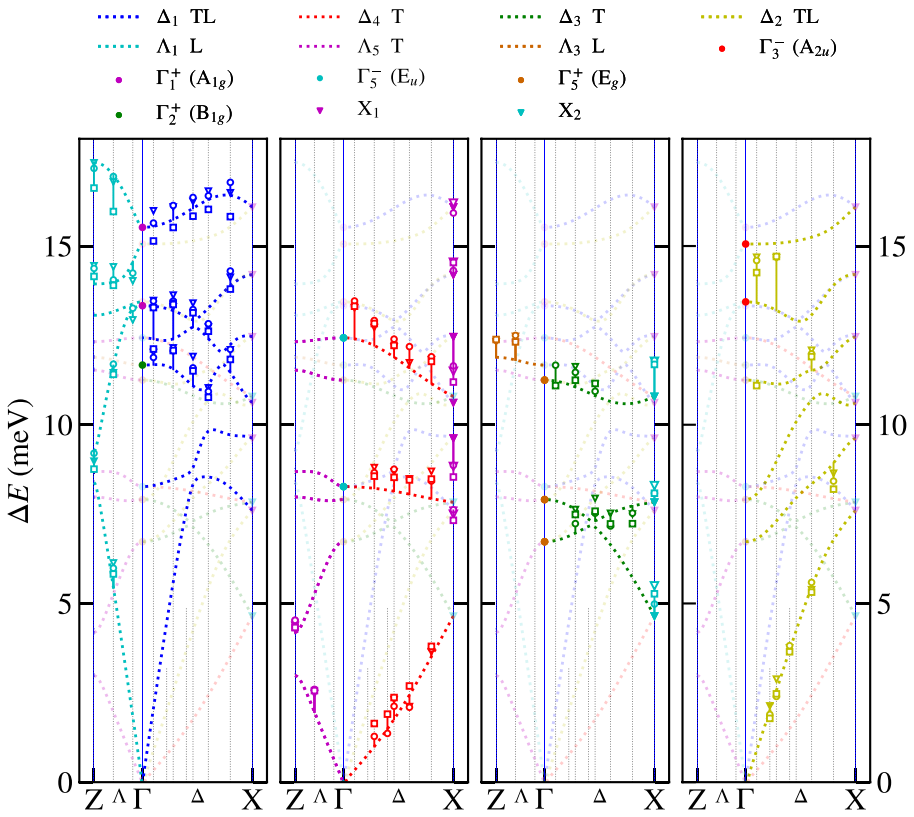

Figure 7. The comparison of theoretical calculation with the fit of measured inelastic X-ray scattering spectra for $LaPd_2Al_2$ in energy range 0 - 17.5 meV. The □, ○, ▽ symbols correspond to 1.5, 80, 300 K, respectively. For details of the fit, see chapter Results - Phonon dispersion curves in (Ce,La)Pd_2Al_2.

solid solution compounds. Also the study of magnetic excitations in the $CeCu_xAl_{4-x}$ system by inelastic neutron scattering[22] shows the continuous evolution of more than three magnetic excitations in the spectra, which is the sign of non-identical Ce environments.

In the case of $CePd_2Al_2$ the relevant phonon modes were suggested to be the A_{1g} modes[5]. We note that the A_{1g} IR transforms as $x^2 + y^2, z^2$ basis functions in the studied symmetry D_{4h}. Only spherical harmonics $Y_{0,0}$ and $Y_{2,0}$ for $l < 9$ transform as A_{1g}, therefore $\hat{O}_\mu$ could be considered as $\tilde{O}_2^0 = 3\hat{J}_z^2 - J(J+1)$ for $CePd_2Al_2$. The situation for reciprocal space points away from the Γ point is more complicated, than in $CeAuAl_3$, because the *P*4/nmm is NSG. The factor group is isomorphic with the point groups only at Γ, Z, V, W points and in the Λ direction. The A_{1g} representation is present only at Z (point group D_{4h}).

Based on these arguments, our experimental study was focused on the A_{1g} modes and on modes in the Δ and Λ directions. There are three A_{1g} modes at Γ point at 12.8, 15.7 and 36.6 meV. Taking into account that the energy of the mode should be comparable to the energy of CEF excitation from the ground state, the mode at 36.6 meV can be excluded. The measurement of related phonon branches to A_{1g} modes at 12.8, 15.7 meV in the vicinity of the Γ point doesn't show any broadening or softening. The other mode symmetries at the Γ point (E_g, E_u, A_{2u}, B_{1g} modes) in the energy interval 7.5–17 meV show a similar temperature dependence as the A_{1g} modes, or their energy is constant in temperature. Looking at the phonon dispersion curves in the Δ and Λ directions, we didn't observed any softening, which also says that in the X and Z points the temperature behaviour is similar. Comparison of raw measured spectra in Supplementary materials of $CePd_2Al_2$ and $LaPd_2Al_2$ homologues show no significant difference, which could be ascribed to the expected quasi-bound state.

The crystal lattice of $CePd_2Al_2$ and $LaPd_2Al_2$ is distorted below 6 K and 60 K, respectively. At 1.5 K, the larger distortion is found for $LaPd_2Al_2$. Therefore we will discuss the influence of distortion on phonon dispersion curves in $LaPd_2Al_2$ homologue. During the distortion we lost the four-fold axis, just two-fold axis remains. This lowering of symmetry leads to decrease of dimension of IRs in mechanical representation. It leads to the splitting of two times degenerated phonon modes at the Γ point ($\Gamma_5^-(E_u)$, $\Gamma_5^+(E_g)$) and also in the Λ direction (Λ_5). On the other hand in the Δ direction the distortion leads only to the modification of their **q** dependencies. In the X point the two fold-degeneracy of phonon modes is kept, because it requires the NSG origin as in the tetragonal case. Fortunately the effect of the distortion is small and the difference is very often smaller than in comparison of Ce and La homologues (see Supplementary information). Therefore we compare the measurement at low temperature with phonon dispersion curves at room temperature in the Figs. 6 and 7 .

We can conclude that our measurements show very good agreement of the observed phonon dispersion curves with the calculated ones without introducing the quasi-bound state. The previous idea[5] that the A_{1g}

phonon modes may be the strongest coupled to the magnetic excitations can be excluded by our study. Other mode symmetries at the Γ point also seem to be unaffected by the quasi-bound state, which opens the question of the meaning of application of a dispersion-less model and even about the presence of a quasi-bound state in $CePd_2Al_2$. Beside $CePd_2Al_2$ we explored the mode symmetries and identified the high symmetry points in the first Brillouin zone of $CeAuAl_3$ and $CeCuAl_3$, at which the following phonon study should be focused in order to follow the consequence of a non-dispersive model of the possible quasi bound state.

Data availibility

Raw data were generated at the SPring-8 large-scale facility. Derived data supporting the findings of this study are available within the article and its Supplementary information for: Lattice dynamics in $CePd_2Al_2$ and $LaPd_2Al_2$.

Received: 3 August 2021; Accepted: 28 September 2021
Published online: 22 October 2021

References

1. Ruminy, M. *et al.* Crystal-field parameters of the rare-earth pyrochlores $R_2Ti_2O_7$ (R = Tb, Dy, and Ho). *Phys. Rev. B* **94**, 024430. https://doi.org/10.1103/PhysRevB.94.024430 (2016).
2. Gaudet, J. *et al.* Magnetoelastically induced vibronic bound state in the spin-ice pyrochlore $Ho_2Ti_2O_7$. *Phys. Rev. B* **98**, 014419. https://doi.org/10.1103/PhysRevB.98.014419 (2018).
3. Loewenhaupt, M. & Steglich, F. The magnetic behaviour of $CeAl_2$ studied by neutron scattering. *Physica B* **88–86**, 187–188. https://doi.org/10.1016/0378-4363(77)90281-9 (1977).
4. Mühle, E., Goremychkin, E. A. & Natkaniec, I. Inelastic Neutron Scattering on (Pr, La)Ni_2 and (Pr, Y)Ni_2. *J. Mag. Mag. Mater.* **81**, 72–78 (1989).
5. Chapon, L. C., Goremychkin, E. A., Osborn, R., Rainford, B. D. & Short, S. Magnetic and structural instabilities in $CePd_2Al_2$ and $LaPd_2Al_2$. *Physica B* **378–380**, 819–820. https://doi.org/10.1016/j.physb.2006.01.300 (2006).
6. Adroja, D. T. *et al.* Vibron Quasibound State in the Noncentrosymmetric Tetragonal Heavy-Fermion Compound $CeCuAl_3$. *Phys. Rev. Lett.* **108**, 216402–1 – 5, https://doi.org/10.1103/PhysRevLett.108.216402 (2012).
7. Čermák, P. *et al.* Magnetoelastic hybrid excitations in $CeAuAl_3$. *Proc. Natl. Acad. Sci. USA* **116**, 6695–6700. https://doi.org/10.1073/pnas.1819664116 (2019).
8. Thalmeier, P. Theory of the bound state between phonons and a CEF excitation in $CeAl_2$. *J. Phys. C: Solid State Phys.* **17**, 4153–4177. https://doi.org/10.1088/0305-4608/14/8/001 (1984).
9. Godet, M., Walker, E. & Purwins, H.-G. Preparation of single crystals of $CeAl_2$ by the Czochralski method. *J. Less-Common Metals* **30**, 301–302. https://doi.org/10.1016/0022-5088(73)90114-8 (1973).
10. Reichardt, W. & Nücker, N. Phonon softening in $CeAl_2$. *J. Phys. F Met. Phys.* **14**, L135–L140. https://doi.org/10.1088/0305-4608/14/8/001 (1984).
11. Tsutsui, S., Kaneko, K., Pospíšil, J. & Haga, Y. Inelastic X-ray scattering of $RTAl_3$ (R = La, Ce, T = Cu, Au). *Physica B* **536**, 24–27. https://doi.org/10.1016/j.physb.2017.09.087 (2018).
12. Legut, D., Diviš, M., Doležal, P., Zhang, S. H. & Javorský, P. Ab initio calculations of the crystal field and phonon dispersions in $CePd_2Al_2$ and $LaPd_2Al_2$. *J. Phys. Condensed Matter* **32**, 235402. https://doi.org/10.1088/1361-648X/ab7031 (2020).
13. Doležal, P. *et al.* Czochralski growth of $LaPd_2Al_2$ single crystals. *J. Crystal Growth* **475**, 10–20. https://doi.org/10.1016/j.jcrysgro.2017.05.016 (2017).
14. Doležal, P. *et al.* Structural instability in $CePd_2(Al, Ga)_2$ and $LaPd_2(Al, Ga)_2$. *J. Alloys Compd.* **790**, 480–492. https://doi.org/10.1016/j.jallcom.2019.02.297 (2019).
15. Baron, A. Q. R. *et al.* An X-ray scattering beamline for studying dynamics. *J. Phys. Chem. Solids* **61**, 461–465. https://doi.org/10.1016/j.jcrysgro.2017.05.016 (2000).
16. Baron, A. Q. R. Phonons in crystals using inelastic X-ray scattering. *J. Spectrosc. Soc. Japan* **58**, 205–2014, arXiv:0910.5764 - english version (2009).
17. Als-Nielsen, J. & McMorrow, D. *Elements of Modern X-ray Physics* (Wiley, 2001).
18. Miller, S. C. & Love, W. F. *Tables of Irreducible Representations of Space Groups and Co-Representations of Magnetic Space Groups* (Pruett Press, 1967).
19. Franz, C. *et al.* Single crystal growth of $CeTAl_3$ (T = Cu, Ag, Au, Pd and Pt). *J. Alloys Comp.* **688**, 978–986. https://doi.org/10.1016/j.jallcom.2016.07.071 (2016).
20. Chlan, V. *et al.* Local atomic arrangement in $LaCuAl_3$ and $LaAuAl_3$ by NMR and density functional theory. *J. Phys. Condens. Matter* **31**, 385601, https://doi.org/10.1088/1361-648X/ab27ac (2019).
21. Matsumura, M., Kawamura, Y., Yoshina, M., Nishioka, T. & Kato, H. ^{27}Al-NQR study in $BaNiSn_3$-type $CeCuAl_3$. *J. Phys. Conf. Ser.* **150**, 042122. https://doi.org/10.1088/1742-6596/150/4/042122 (2009).
22. Klicpera, M. *et al.* Magnetic structure and excitations in $CeCu_xAl_{4-x}$ system. *Inorganic Chem.* **56**, 12839–12847. https://doi.org/10.1021/acs.inorgchem.7b01521 (2017).

Acknowledgements

This work was supported by the following projects: Czech Science Foundation under Grant No. 17-04925J, ERDF in the IT4Innovations & Nanotechnology Center, CEET, VSB national supercomputing center - path to exascale project (CZ.02.1.01/0.0/0.0/16_013/0001791) within the OPRDE and the project e-INFRA CZ (ID:90140) by the Ministry of Education, Youth and Sports of the Czech Republic, by the project NanoCent-Nanomaterials centre for advanced applications, project No. CZ.02.1.01/0.0/0.0/15_003/0000485, financed by the ERDF and projects JSPS KAKENHI (Grant Nos. JP16K05031, JP19H04408, JP20H01864). The inelastic X-ray scattering experiments were performed under the approval of JASRI (proposal No. 2018A1676, 2018B1705) and financially supported by the "Budding Researchers Support" program of JASRI. Sample preparation and characterisation was performed in MGML (http://mgml.eu/), which was supported within the program of Czech Research Infrastructures (project no. LM2018096). We thank Adam Bartoš, Petr Čermák and Milan Klicpera for valuable discussion and Ross Harvey Colman for proofreading the article.

Author contributions

P.J. supervised the research. P.D., K.C. and P.J. wrote the manuscript. P.D. analysed the experimental data and performed the symmetry analysis of phonon modes. P.C., S.T., K.K. and P.D. performed the experimental

measurements. D.L. performed the theoretical calculation of phonon dispersion curves. P.C. performed the simulation of the scattering intensity based on the dynamical structure factor.

Competing interests
The authors declare no competing interests.

Additional information
Supplementary Information The online version contains supplementary material available at https://doi.org/10.1038/s41598-021-99904-7.

Correspondence and requests for materials should be addressed to P.D.

Reprints and permissions information is available at www.nature.com/reprints.

Publisher's note Springer Nature remains neutral with regard to jurisdictional claims in published maps and institutional affiliations.